Fundamental limits on shape estimation

Alfred Hero

University of Michigan - Ann Arbor

`http://www.eecs.umich.edu/~hero/hero.html`

Students: Jia Li and Robinson Piramuthu

Outline

- ➥ Resolution–limited imaging problem
- ➥ Parametric shape model
- ➥ Minimum achievable estimator variance: the CR bound
- ➥ Bound sensitivity and extremal shapes
- ➥ Numerical comparisons

Resolution Limited Imaging Problem

Two-level Image Model

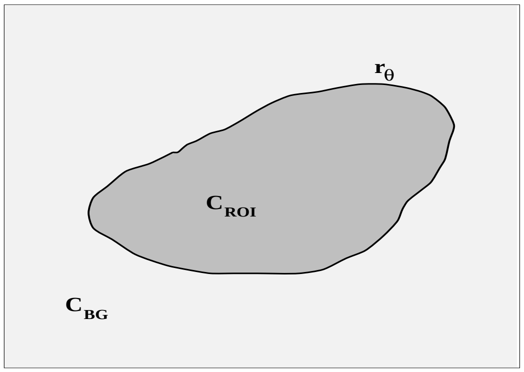

An arbitrary two–level image containing boundary curve $\boldsymbol{r}_{\tilde{\boldsymbol{\theta}}}$

❖ **Notation:**

$$
\begin{aligned}
\mathrm{I}_{\tilde{\boldsymbol{\theta}}}(x,y) &= \text{True image} \\
\tilde{\boldsymbol{\theta}} &= \text{Parameterization of boundary of object} \\
\mathrm{I}_{R_{\tilde{\boldsymbol{\theta}}}} &= \text{Indicator function for the object } R_{\tilde{\boldsymbol{\theta}}} \\
C_{\mathrm{INT}} &= \text{Uniform intensity of interior of } R_{\tilde{\boldsymbol{\theta}}} \\
C_{\mathrm{BG}} &= \text{Uniform intensity of background} \\
\mathrm{I}_{\tilde{\boldsymbol{\theta}}}(x,y) &= C_{\mathrm{INT}} \cdot \mathrm{I}_{R_{\tilde{\boldsymbol{\theta}}}}(x,y) + C_{\mathrm{BG}} \cdot (1 - \mathrm{I}_{R_{\tilde{\boldsymbol{\theta}}}}(x,y)).
\end{aligned}
$$

Measurement Statistics

- **Observation Model:**

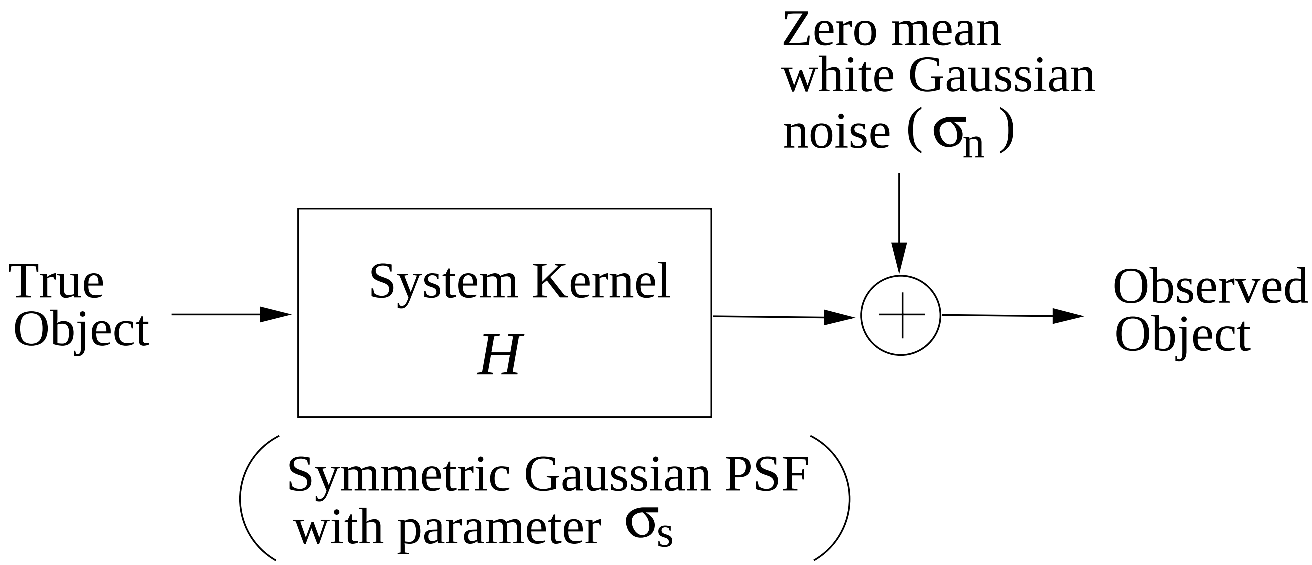

- $$H(x,y) = \frac{1}{2\pi\sigma_n^2} \exp\left\{-\frac{x^2+y^2}{2\sigma_s^2}\right\}$$
$$n(x,y) \sim \mathcal{N}(0,\sigma_n^2)$$
$$\boldsymbol{Y}_{\mathrm{M}}(x,y) = (I_{\tilde{\boldsymbol{\theta}}} ** H)(x,y) + n(x,y).$$

Parametric Shape Model

- ➥ For 2–D shape: polar boundary representation $\boldsymbol{r_\theta}(\psi)$.
- ➥ For 3–D shape: spherical boundary representation $\boldsymbol{r_\theta}(\alpha, \beta)$

Assume :

❶ Boundary is star–shaped.

❷ Center of description is fixed.

Star–shapes in 2–D

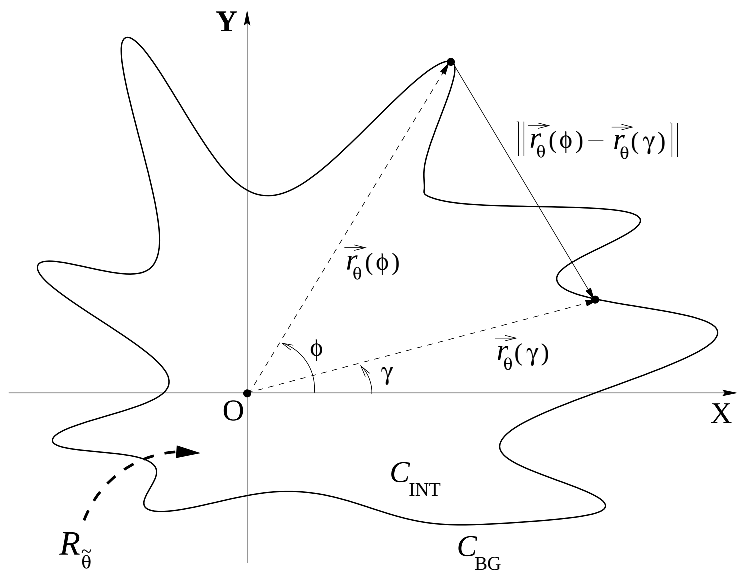

(a) Star–Shaped

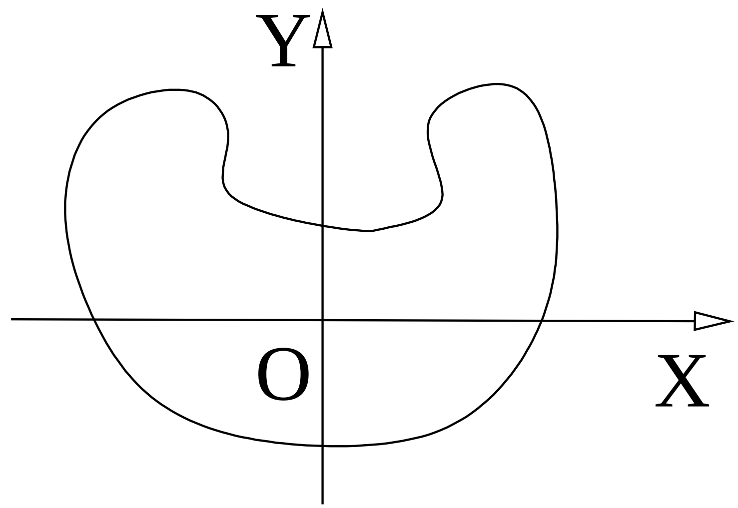

(b) Not Star–Shaped

Examples: B-splines, Fourier descriptors, Bezier curves, ...

Measurement Degradation

❖ Flower–shaped object (16 knots)

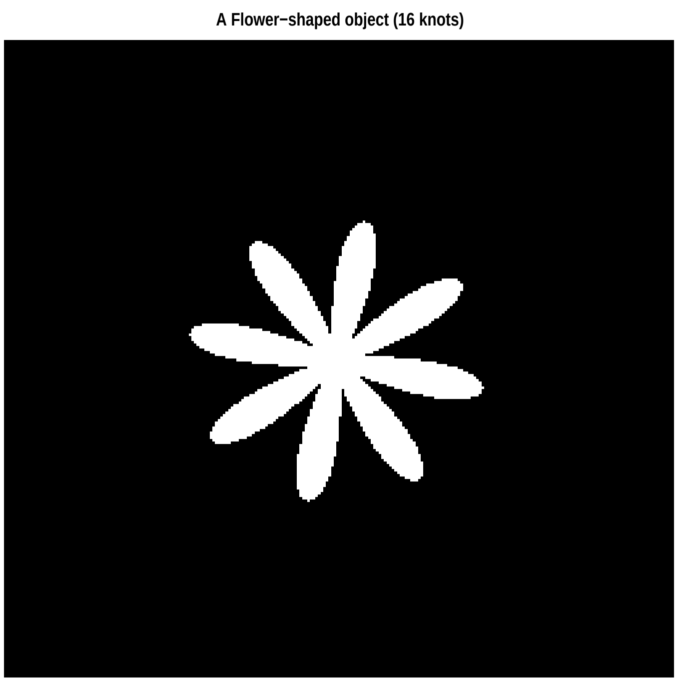

(c) True

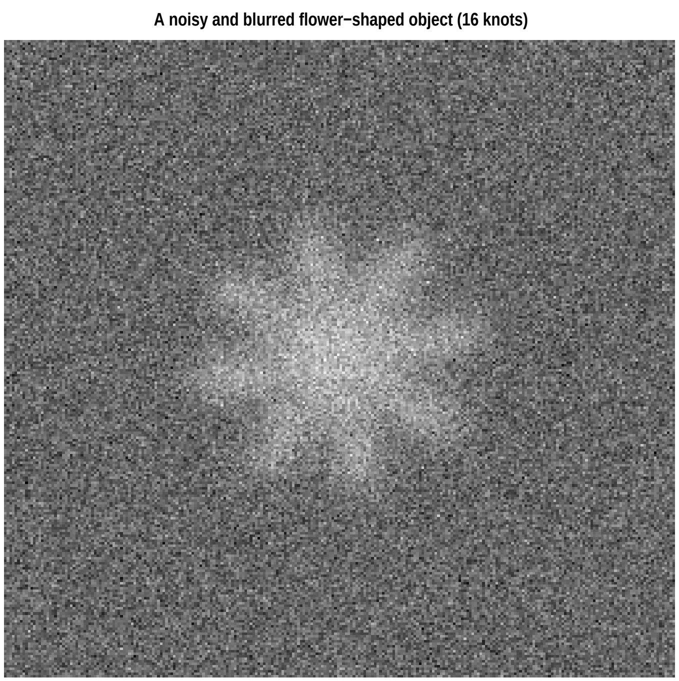

(d) Observed

Finite dimensional parameterization: B–splines

❖ Polar parameterization by periodic B–splines with a fixed number K of knots.

❖ **Notation:**

$$\begin{aligned} \boldsymbol{\theta} &= \text{B–spline coefficients} \\ B_i(\phi) &= i\text{–th B–spline basis at angle } \phi \\ r_{\boldsymbol{\theta}}(\phi) &= \sum_{i=1}^{K} \theta_i B_i(\phi) = \boldsymbol{B}^T(\phi)\boldsymbol{\theta} \quad \text{(radial samples).} \end{aligned}$$

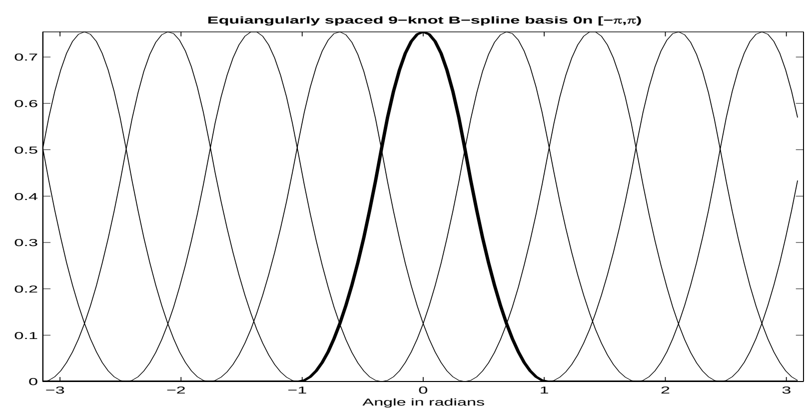

The periodic cubic B–spline basis functions for an equiangularly spaced set of 9 knots on domain $[-\pi, \pi]$.

CR Bound

- Cramèr–Rao lower bound:

For any unbiased estimator $\hat{\boldsymbol{\theta}}$ *of parameter vector* $\boldsymbol{\theta}$*:*

$$\operatorname{cov}_{\boldsymbol{\theta}}\left(\hat{\boldsymbol{\theta}}\right) \geq F_{\boldsymbol{\theta}}^{-1}$$

where $F_{\boldsymbol{\theta}}$ *is Fisher information matrix*

$$F_{\boldsymbol{\theta}} = E_{\boldsymbol{\theta}}\left[-\nabla^2 \log f(\boldsymbol{Y}_M|\boldsymbol{\theta})\right]$$

Fisher Information Matrix for 2–D

$$\boldsymbol{F}_{\boldsymbol{\theta}} = C_{\mathrm{CN}} \iint_{-\pi}^{\pi} \exp\left[-\frac{\|\vec{r}_{\boldsymbol{\theta}}(\phi) - \vec{r}_{\boldsymbol{\theta}}(\gamma)\|^2}{4\sigma_s^2}\right] r_{\boldsymbol{\theta}}(\phi)\, r_{\boldsymbol{\theta}}(\gamma)\, \boldsymbol{B}(\phi)\, \boldsymbol{B}^T(\gamma)\, d\phi\, d\gamma \tag{1}$$

where

$$C_{\mathrm{CN}} = \frac{(C_{\mathrm{INT}} - C_{\mathrm{BG}})^2}{4\pi\sigma_n^2\sigma_s^2} = \frac{(contrast)^2}{4\pi\sigma_n^2\sigma_s^2}$$

Asymptotic Fisher Information for 2–D

- **Define:**

$$h_{\boldsymbol{\theta}}(\psi) = \frac{r_{\boldsymbol{\theta}}^2}{\sqrt{r_{\boldsymbol{\theta}}^2(\psi) + \left[r_{\boldsymbol{\theta}}'(\psi)\right]^2}}$$

and

$$\sigma_m = \max_{\phi} \left\{ \frac{\sqrt{2}\sigma_s}{\left|\left|\vec{r}_{\boldsymbol{\theta}}'(\phi)\right|\right|} \right\}$$

- **Then:**

$$\boldsymbol{F}_{\boldsymbol{\theta}} = \frac{(contrast)^2}{2\sqrt{\pi}\sigma_s\sigma_n^2} \cdot \int_{-\pi}^{\pi} h_{\boldsymbol{\theta}}(\psi)\ \boldsymbol{B}(\psi)\boldsymbol{B}^T(\psi)d\psi + o(\sigma_m)$$

Geometrical Interpretation: 2–D

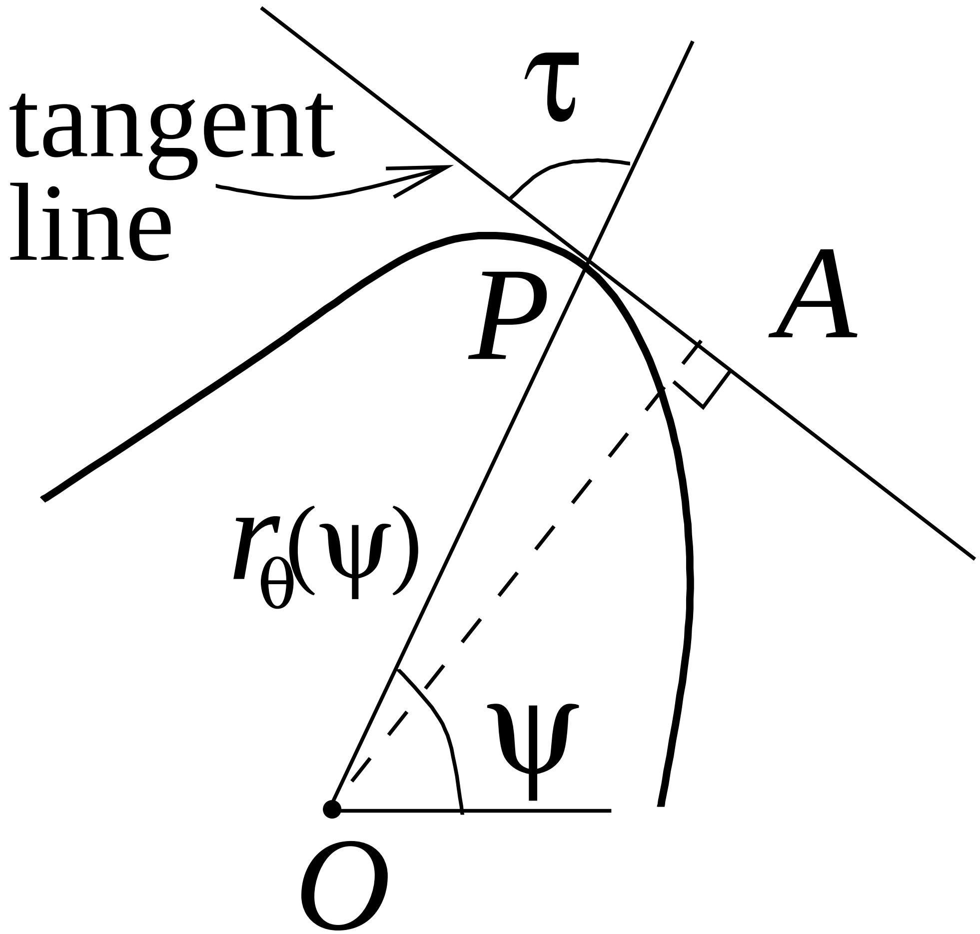

Figure 1: Relation between tangent line and $h_{\boldsymbol{\theta}}(\psi)$.

Fisher Information Matrix for 3–D

$$\boldsymbol{F}_{\boldsymbol{\theta}} \quad = \quad C_{\mathrm{CN}} \cdot \int_{-\frac{\pi}{2}}^{\frac{\pi}{2}} \int_{-\pi}^{\pi} \int_{-\frac{\pi}{2}}^{\frac{\pi}{2}} \int_{-\pi}^{\pi} \exp\left(\frac{\|\vec{r}_{\boldsymbol{\theta}}(\alpha_1, \beta_1) - \vec{r}_{\boldsymbol{\theta}}(\alpha_2, \beta_2)\|^2}{-4\sigma_s^2} \right)$$

$$\boldsymbol{r}_{\boldsymbol{\theta}}^2(\alpha_1, \beta_1)\, \boldsymbol{r}_{\boldsymbol{\theta}}^2(\alpha_1, \beta_2) \cdot\ \boldsymbol{B}(\alpha_1, \beta_1); \boldsymbol{B}^T(\alpha_2, \beta_2)\ \cos\alpha_1 \cos\alpha_2\, d\alpha_1\, d\beta_1\, d\alpha_2\, d\beta_2$$

where

$$C_{\mathrm{CN}} := \frac{(C_{\mathrm{INT}} - C_{\mathrm{BG}})^2}{8\pi^{3/2}\sigma_s^3\sigma_n^2} = \frac{\mathrm{contrast}^2}{8\pi^{3/2}\sigma_s^3\sigma_n^2}.$$

Asymptotic Fisher Information for 3–D

- **Define:**

$$h_{\boldsymbol{\theta}}(\alpha,\beta) = \frac{\boldsymbol{r}_{\boldsymbol{\theta}}^{3}(\alpha,\beta)}{\sqrt{\left[\boldsymbol{r}_{\boldsymbol{\theta}}{}^{10}(\alpha,\beta)\right]^2 + \left[\boldsymbol{r}_{\boldsymbol{\theta}}{}^{01}(\alpha,\beta)\right]^2 + \boldsymbol{r}_{\boldsymbol{\theta}}^{2}(\alpha,\beta)}}.$$

- **Then:**

$$\boldsymbol{F}_{\boldsymbol{\theta}} = 4\pi C_{\mathrm{CN}}\sigma_s^2 \int_{\alpha=-\frac{\pi}{2}}^{\frac{\pi}{2}} \int_{\beta=-\pi}^{\pi} h_{\boldsymbol{\theta}}(\alpha,\beta)\,\boldsymbol{B}(\alpha,\beta)\boldsymbol{B}^T(\alpha,\beta)\,\cos^2\alpha\,d\alpha\,d\beta$$

$$+o(\sigma_m)$$

Geometrical Interpretation: 3–D

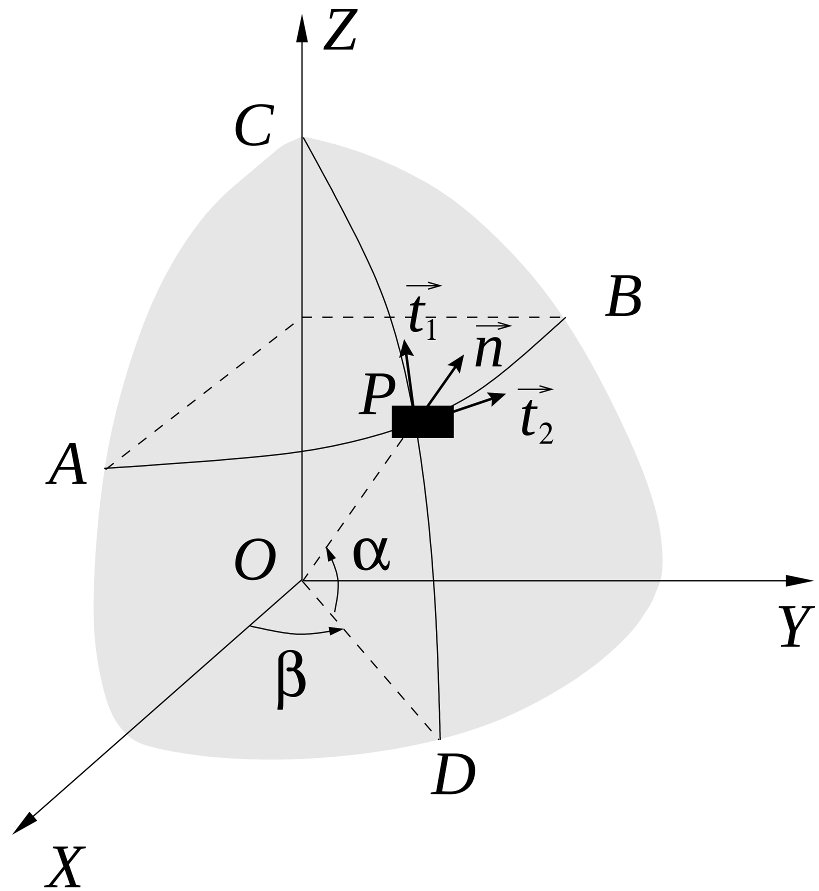

Figure 2: Unit tangent and normal vectors for a spherical surface through P. Here, O is the center of the sphere as well as the center–of–description.

Optimum Center of Description

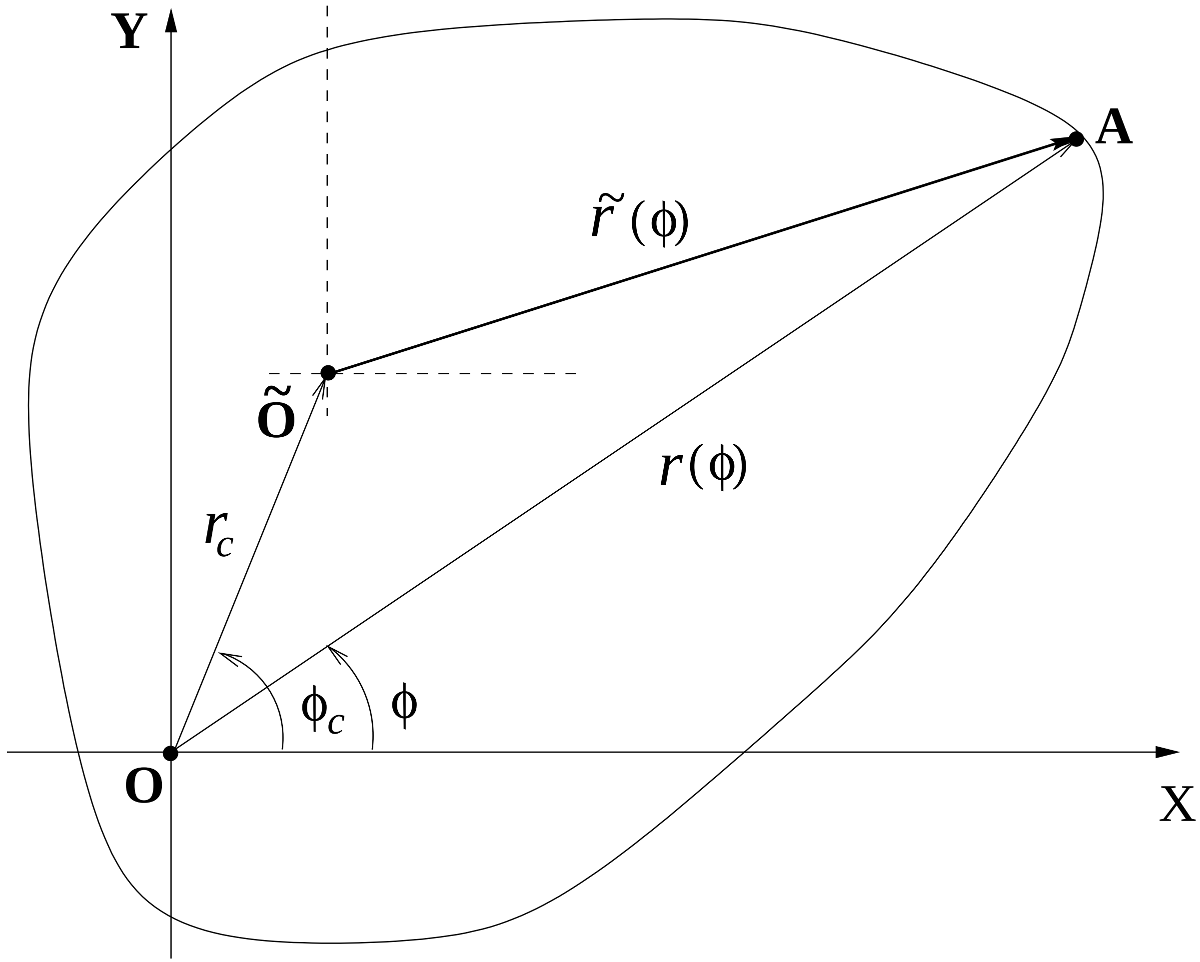

Figure 3: Change of center–of–description.

Optimum Center of Description: example

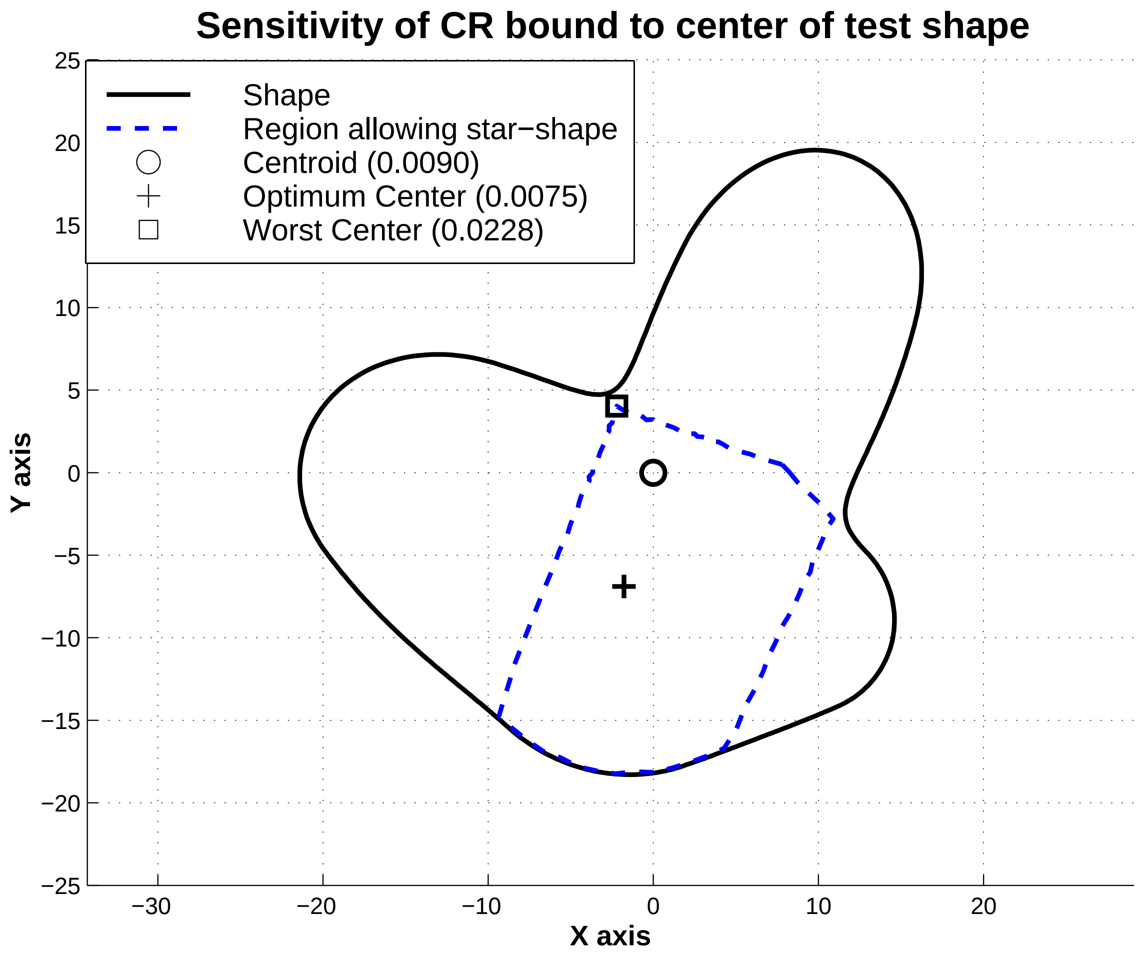

Figure 4: Sensitivity of CR bound to shift in center–of–description of a test shape.

Worst–Case 2–D Shape Analysis via FIM

- Consider minimization of

$$\text{trace}\{\boldsymbol{F_\theta}\} = C \int_{\phi=-\pi}^{\pi} h_{\boldsymbol{\theta}}(\phi)\, f_B(\phi) d\phi \qquad (2)$$

where $C = \frac{(contrast)^2}{2\sqrt{\pi}\sigma_s \sigma_n^2}$ and

$$f_B(\phi) = \boldsymbol{B}^T(\phi)\boldsymbol{B}(\phi) = \sum_{i=1}^{K} B_i^2(\phi).$$

- under fixed perimeter constraint

$$P = \int_{\phi=-\pi}^{\pi} \sqrt{[\boldsymbol{r_\theta}(\phi)]^2 + [\boldsymbol{r'_\theta}(\phi)]^2} d\phi = 1. \qquad (3)$$

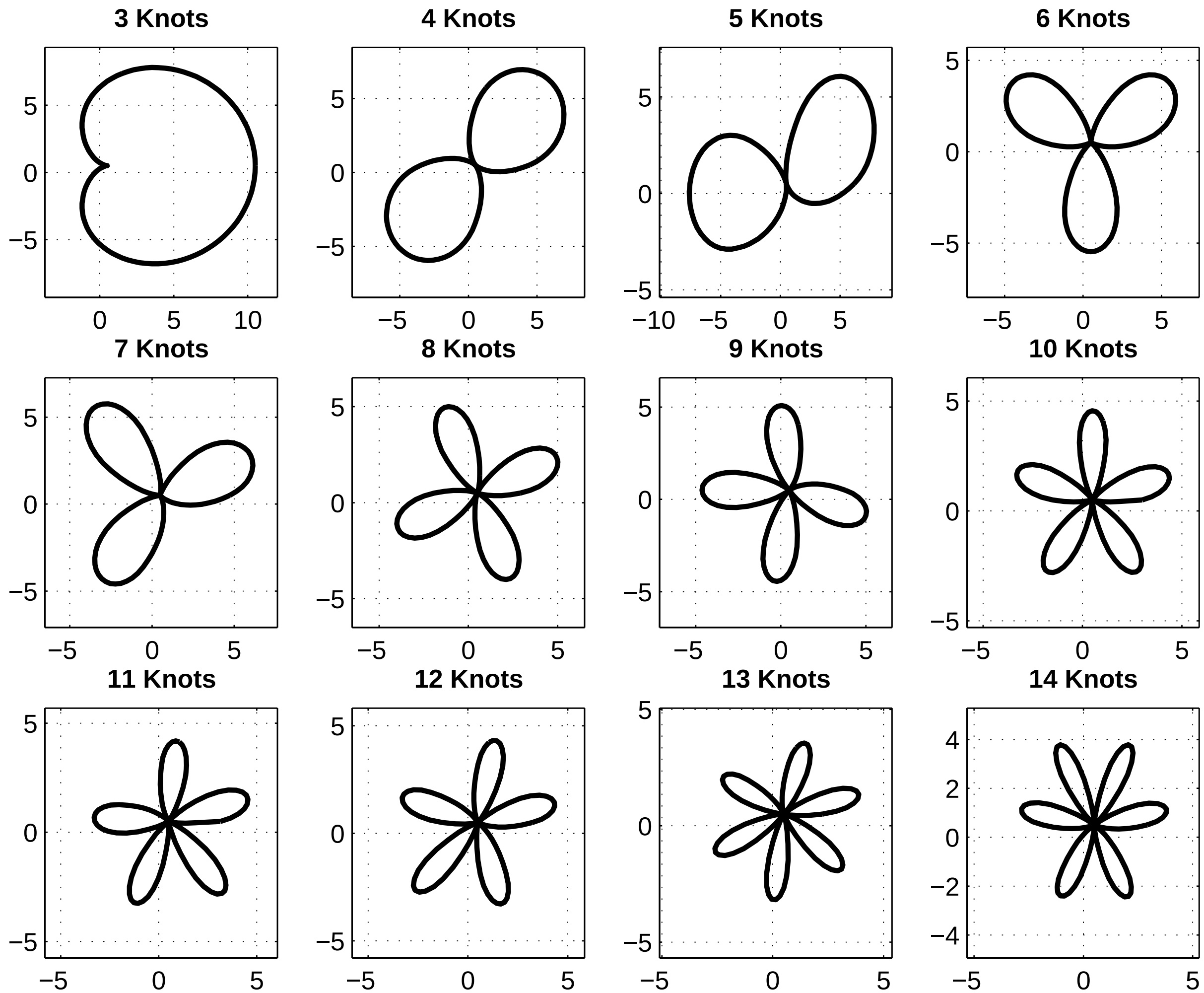

Figure 5: Collection of worst shapes on quadratic B–splines basis.

Worst–Case Nearly Circular 2–D Shapes

- circularity measure:

$$\gamma = \frac{4\pi A}{P^2} = \frac{4\pi \int_{\phi=-\pi}^{\pi} \boldsymbol{r}_{\boldsymbol{\theta}}^2(\phi) d\phi}{\left(\int_{\phi=-\pi}^{\pi} \sqrt{[\boldsymbol{r}_{\boldsymbol{\theta}}(\phi)]^2 + [\boldsymbol{r}'_{\boldsymbol{\theta}}(\phi)]^2} d\phi \right)^2}$$

where $\gamma \in [0,1]$

- Lagrangian for: max trace$\{\boldsymbol{F}_{\boldsymbol{\theta}}\}$ s.t. $\gamma \geq 1 - \epsilon$, $P = 1$

$$\boldsymbol{L(\theta) = a_f^T \theta - \frac{1}{2} \theta^T D_f \theta + \lambda_1 \theta^T Q \theta + \lambda_2 (a^T \theta + \frac{1}{2} \theta^T D \theta)}$$

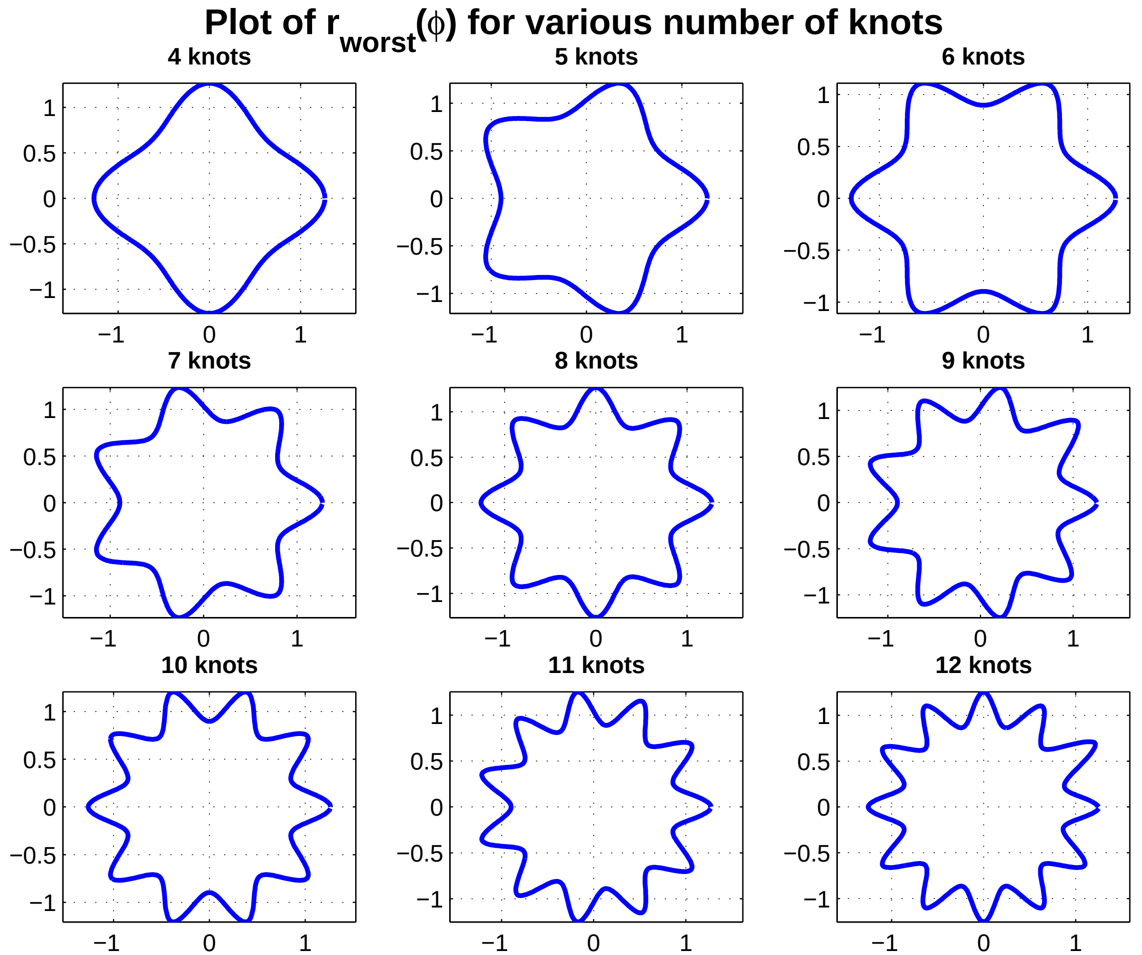

Figure 6: Worst–shapes local to a circle for finite dimensional case with quadratic B–splines and equally spaced knots.

Worst–Case Nearly Spherical 3–D Shapes

- sphericity measure $\gamma \in [0,1]$:

$$\gamma \quad = \quad \frac{36\pi S^3}{V^2} =$$

$$\frac{36\pi \left(\int \sqrt{[\boldsymbol{r}_{\boldsymbol{\theta}}(\alpha,\beta)]^2 + [\boldsymbol{r}_{\boldsymbol{\theta}}^{10}(\alpha,\beta)]^2 + [\boldsymbol{r}_{\boldsymbol{\theta}}^{01}(\alpha,\beta)]^2} \ \ \boldsymbol{r}_{\boldsymbol{\theta}}(\alpha,\beta)\cos(\alpha) d\alpha d\beta \right)^3}{\left(\int_{-\pi/2}^{\pi/2} \int_{-\pi}^{\pi} \boldsymbol{r}_{\boldsymbol{\theta}}^3(\alpha,\beta)\cos(\alpha) d\alpha d\beta \right)^2}$$

- Lagrangian for max trace$\{\boldsymbol{F}_{\boldsymbol{\theta}}\}$ s.t. $\gamma \geq 1-\epsilon$, $P=1$

$$\boldsymbol{L(\theta) = \theta^T [Q_f - \frac{1}{2} D_f] \theta + \lambda_1 (\theta^T Q \theta - a^T \theta) + \lambda_2 (\frac{1}{2} \theta^T [D+Q] \theta + a^T \theta)}$$

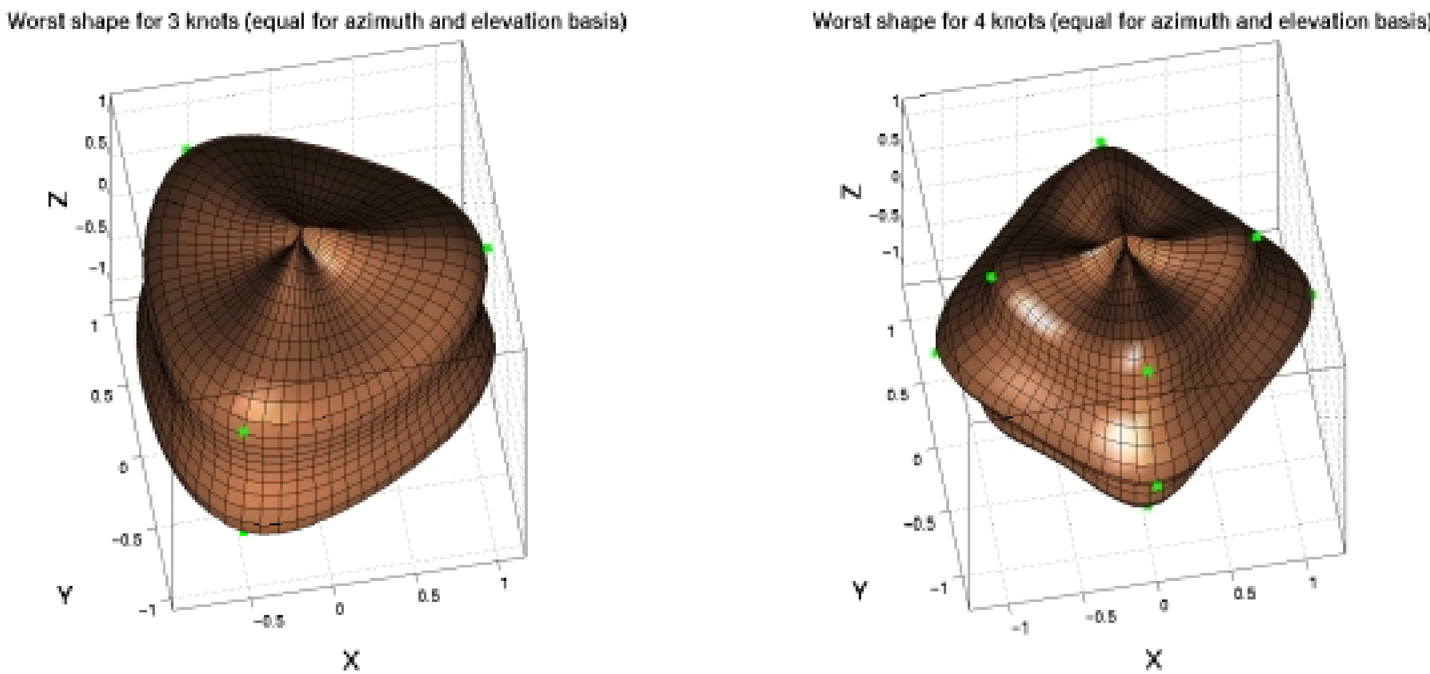

(a) 3 × 3 Knots

(b) 4 × 4 Knots

Figure 7: Worst–shapes local to a sphere.

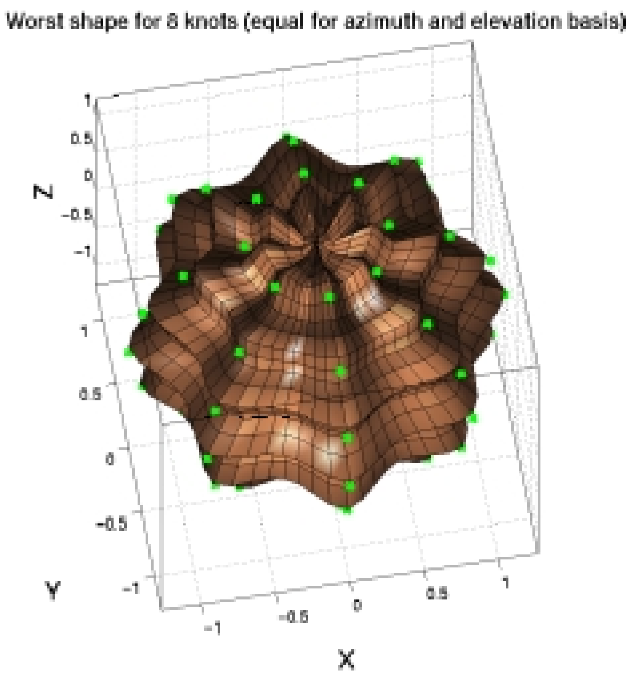

(a) 8 × 8 Knots

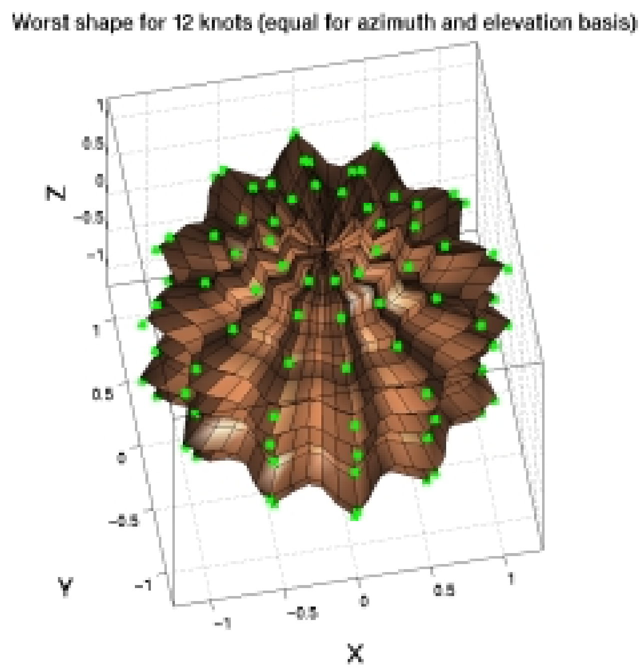

(b) 12 × 12 Knots

Figure 8: Worst–shapes local to a sphere.

Edge Filtering Technique

1. Transform observed data from cartesian coordinates to spherical coordinates.
2. Apply edge filter ($[-1, \ldots, -1, 1, \ldots, 1]$) along each angle and extract edge.
3. Apply a 2 x 2 median filter to this extracted surface of radial values.

Drawbacks:

- Bias due to system PSF.
- Sensitive to noise.

Edge Filtering Technique (contd.)

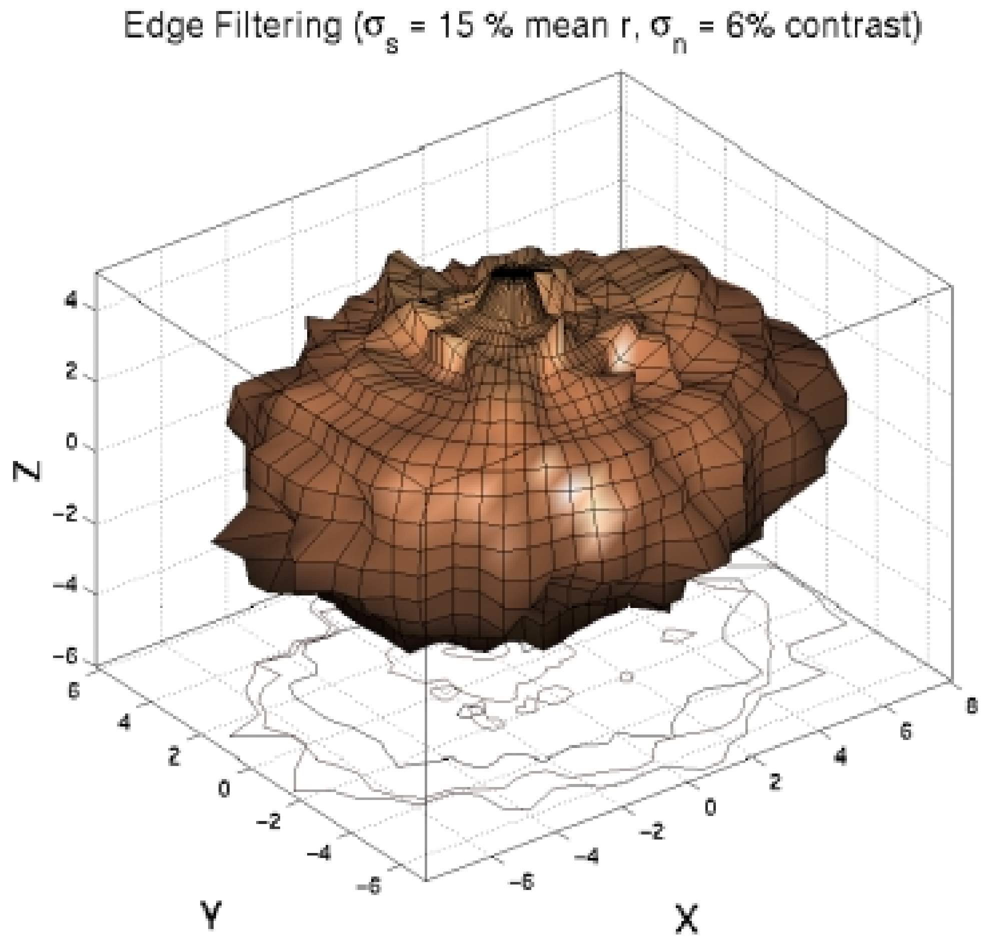

Edge Filtering Technique + Projection on B–Spline Basis

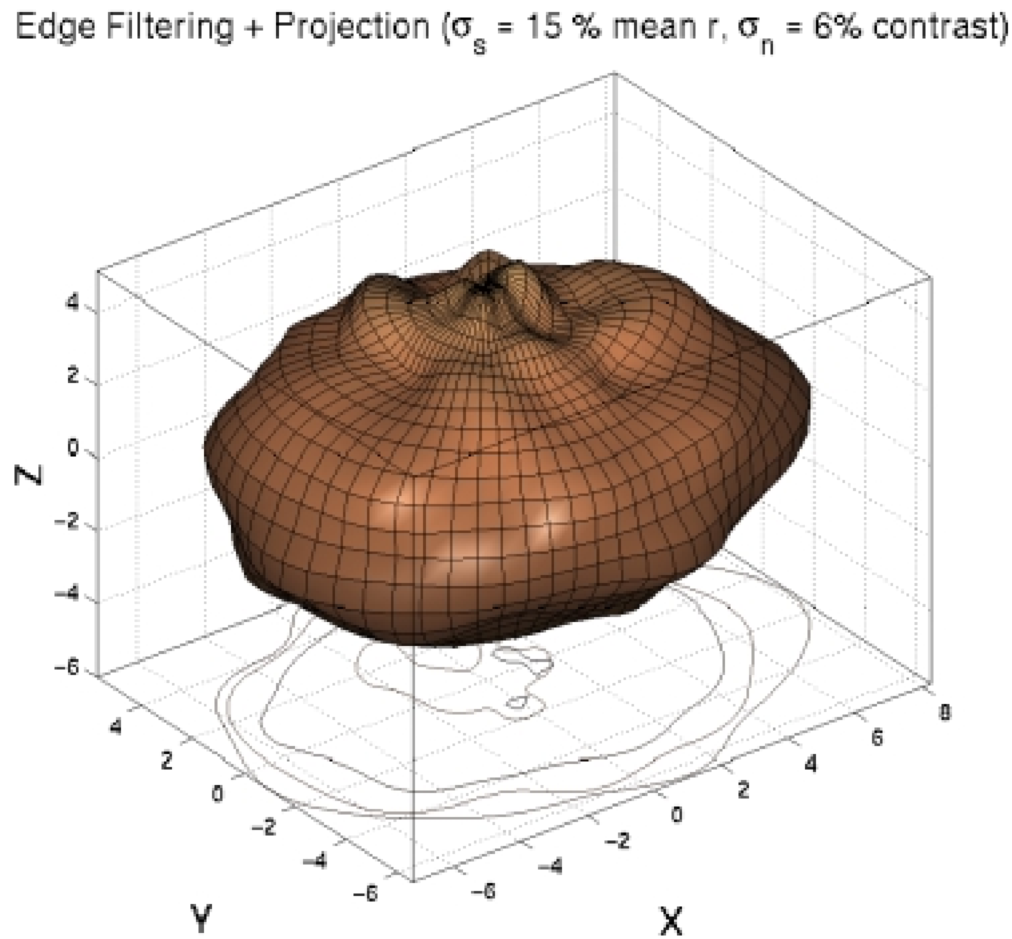

Empirical Bias as a Function of σ_s

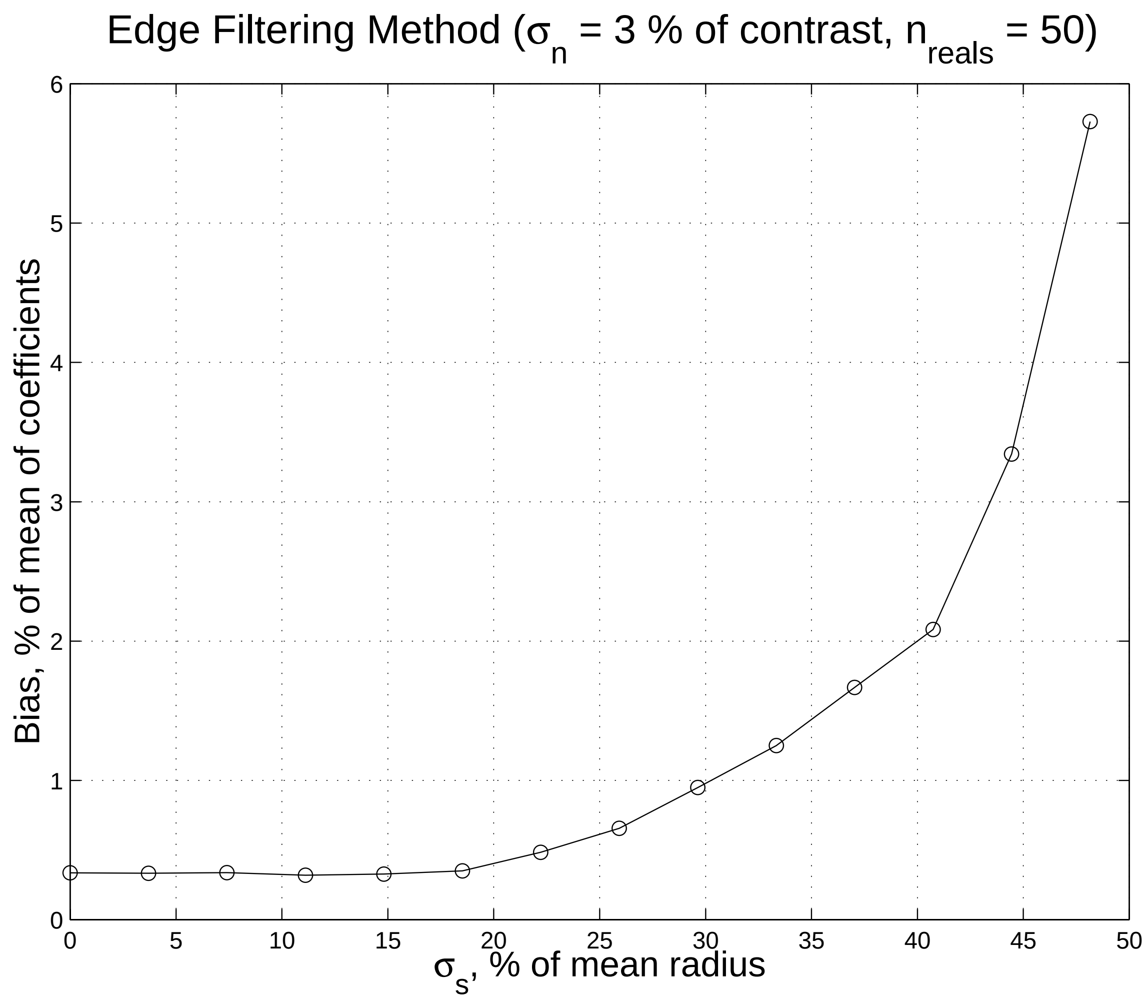

Empirical Bias as a Function of σ_n

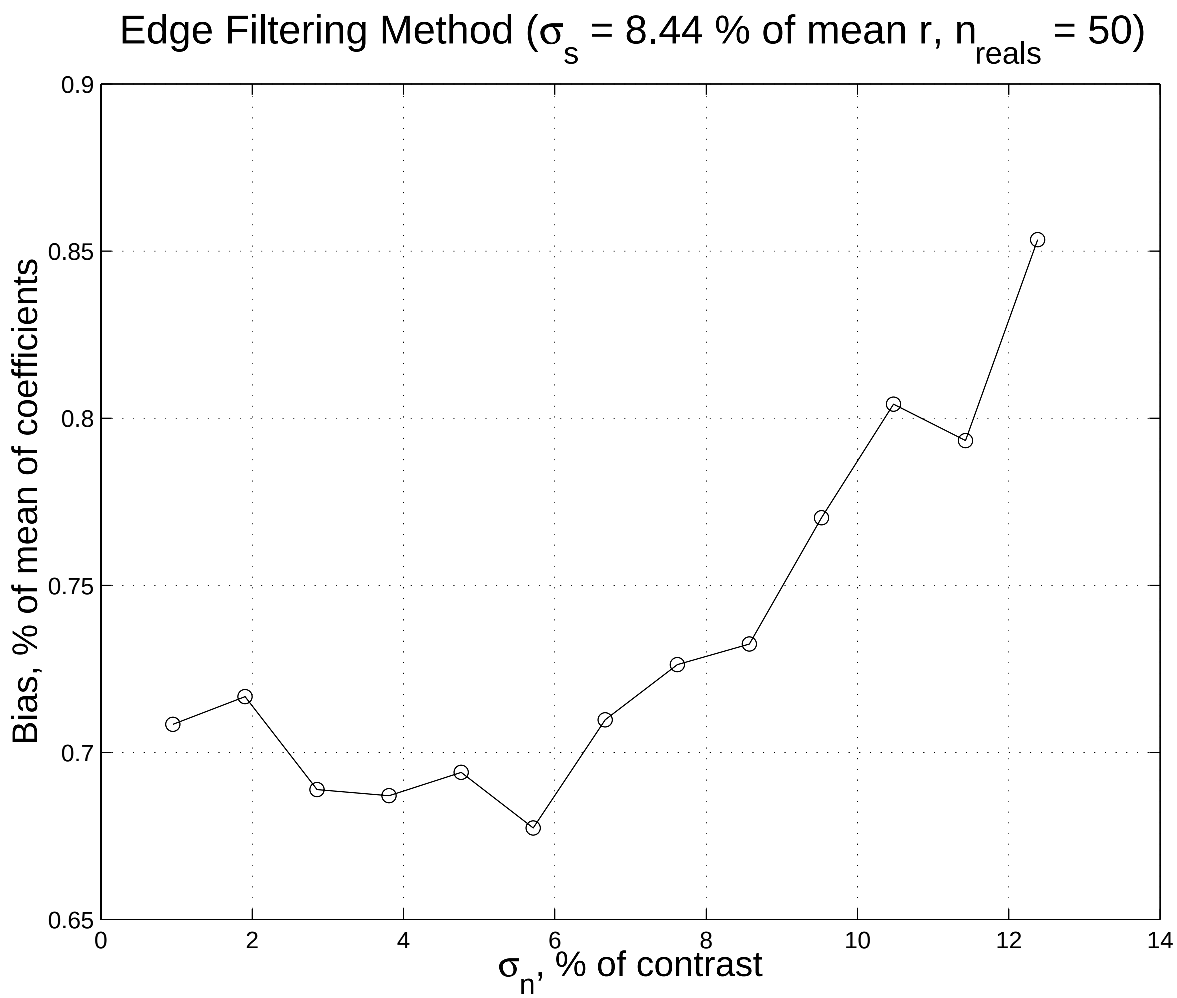

Empirical Standard Deviation as a Function of σ_s

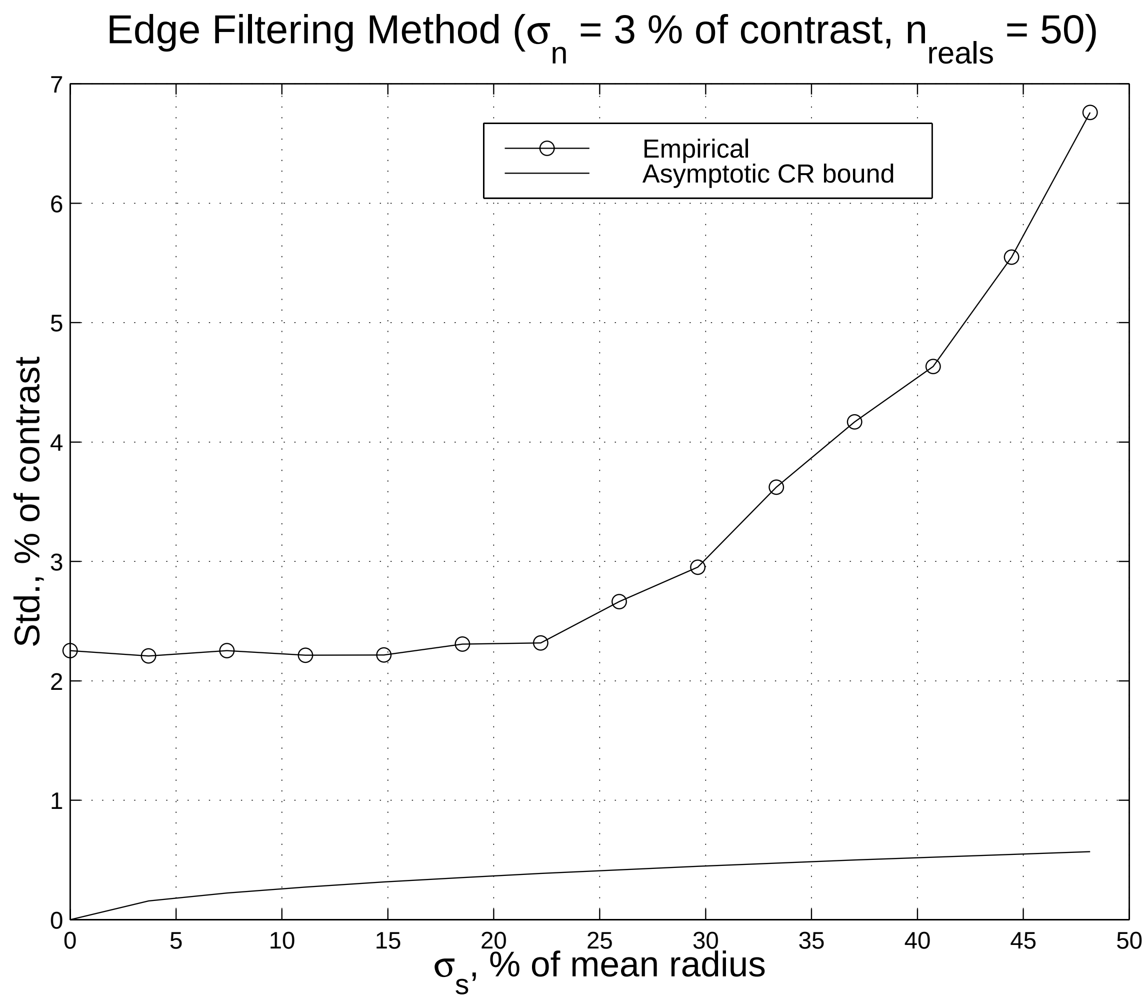

Empirical Standard Deviation as a Function of σ_n

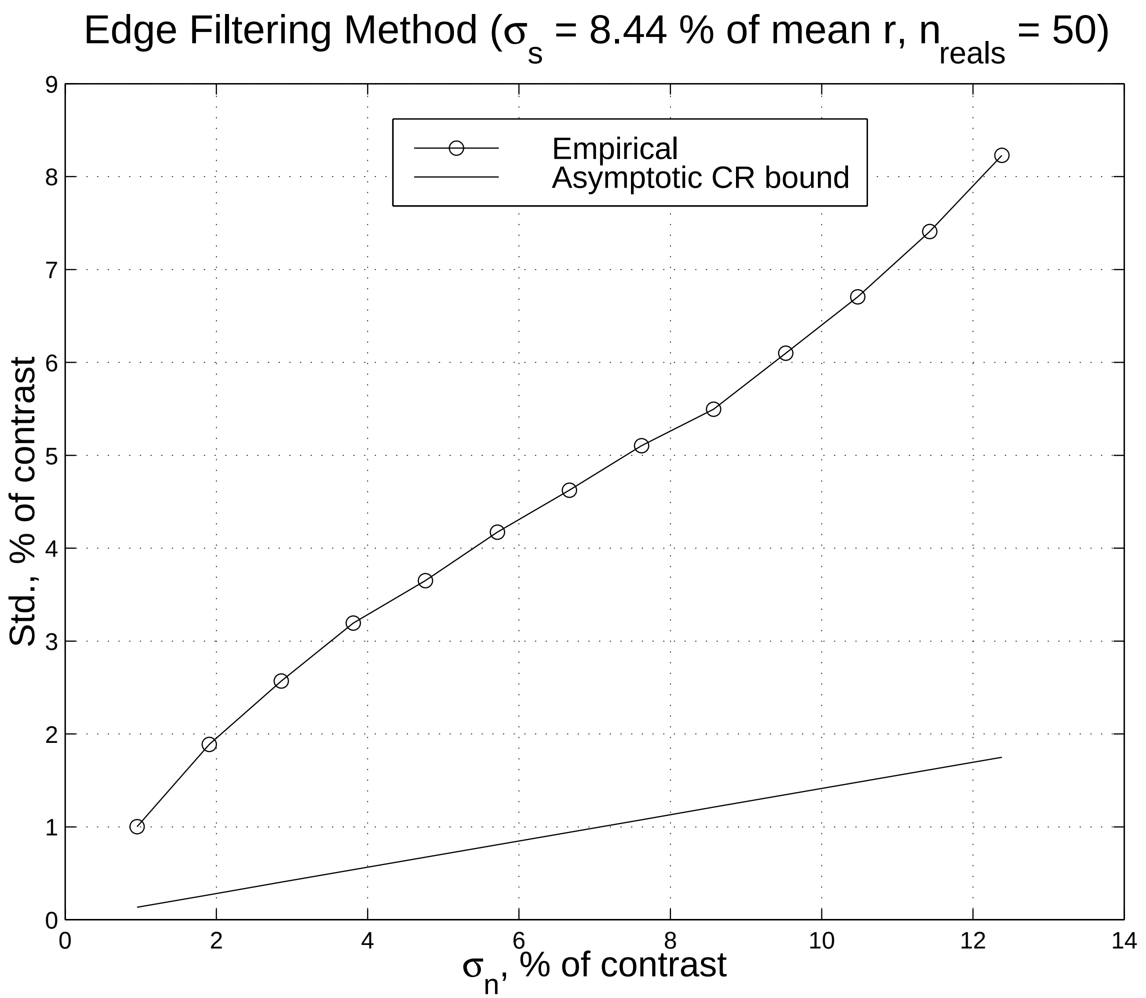

Conclusions

❶ CR bound permits study of sensitivity of minimum achievable boundary estimation error

❷ Approach has been applied to

- MRI-aided PET: Fisher information = confidence of side info
- Analysis of lung nodule quantification in ECT
- PET/CT/MRI image registration studies
- Assessment of ML, active contour, and edge filtering methods of shape estimation

❸ Method restricted to star shaped objects